

TITLE: GAMMA-RAY MEASUREMENTS AT THE WNR WHITE NEUTRON SOURCE

AUTHOR(S): Ronald O. Nelson, Stephen A. Wender, and Douglas R. Mayo

SUBMITTED TO: NEANC Specialist's Meeting on Measurement, Calculation  
and Evaluation of Photon  
Bologna, Italy  
November 9-11, 1994

By acceptance of this article, the publisher recognizes that the U.S. Government retains a non-exclusive, royalty-free license to publish or reproduce the published form of this contribution, or to allow others to do so, for U.S. Government purposes.

The Los Alamos National Laboratory requests that the publisher identify this article as work performed under the auspices of the U.S. Department of Energy.

---

Los Alamos

Los Alamos National Laboratory  
Los Alamos, New Mexico 87545

**MASTER**

DISTRIBUTION OF THIS DOCUMENT IS UNLIMITED

## **DISCLAIMER**

This report was prepared as an account of work sponsored by an agency of the United States Government. Neither the United States Government nor any agency thereof, nor any of their employees, makes any warranty, express or implied, or assumes any legal liability or responsibility for the accuracy, completeness, or usefulness of any information, apparatus, product, or process disclosed, or represents that its use would not infringe privately owned rights. Reference herein to any specific commercial product, process, or service by trade name, trademark, manufacturer, or otherwise does not necessarily constitute or imply its endorsement, recommendation, or favoring by the United States Government or any agency thereof. The views and opinions of authors expressed herein do not necessarily state or reflect those of the United States Government or any agency thereof.

## **DISCLAIMER**

**Portions of this document may be illegible in electronic image products. Images are produced from the best available original document.**

## GAMMA-RAY MEASUREMENTS AT THE WNR WHITE NEUTRON SOURCE

R.O. Nelson, S.A. Wender, and D.R. Mayo

*P-23, M.S. H803, Los Alamos National Laboratory, Los Alamos, NM 87545, U.S.A.*

### ABSTRACT

Photon production data have been acquired in the incident neutron energy range,  $1 < E_n < 400$  MeV, for a number of target nuclei, gamma-ray energy ranges, and reactions, using the continuous-energy neutron beam of the WNR facility at Los Alamos. Gamma-ray production measurements using high resolution Ge detectors have been employed for gamma-rays in the energy range,  $0.1 < E_\gamma < 10$  MeV. These measurements allow identification of reactions from the known energies of the gamma-ray transitions between low-lying states in the final nucleus. Some of the targets studied include: N, O, Al, Na,  $^{56}\text{Fe}$ , and  $^{207,208}\text{Pb}$ . These data are useful both for testing nuclear reaction models at intermediate energies and for numerous applied purposes. BGO detectors do not have the good energy resolution of Ge detectors, but have much greater detection efficiency for gamma rays with energies greater than a few MeV. We have used an array of 5 BGO detectors to measure cross sections and angular distributions for photon production from C and N. A large, well-shielded BGO detector has been used to measure fast neutron capture in the giant resonance region with a maximum gamma-ray energy of 52 MeV. We present results of our study of the isovector giant quadrupole resonance in  $^{41}\text{Ca}$  via these capture measurements. Recent measurements of inclusive photon spectra from our neutron proton Bremsstrahlung experiment have been made using a gamma-ray telescope to detect gamma-rays in the energy range,  $40 < E_\gamma < 300$  MeV. This detector is briefly described. The advantages and disadvantages of these detector systems are discussed using examples from our measurements. The status of current measurements is presented.

### 1. Introduction

The WNR spallation neutron source at Los Alamos provides intense beams of neutrons with energies spanning the range from less than 1 MeV to more than 400 MeV. The continuous energy coverage enables simultaneous measurements of detailed excitation functions in the neutron energy range below 20 MeV, which is of great interest in many applied areas such as providing reaction cross sections needed for reactor shielding. The wide energy range allows us to simultaneously extend our measurements to intermediate energies for which very little data has been available in the past. These intermediate energy data are of interest in testing and extending reaction theory to higher energies, and also have practical applications such as in microdosimetry for neutron radiotherapy and in shielding for space missions where cosmic ray induced neutrons can provide a significant fraction of the dose.

Since the beginning  $\gamma$ -ray measurements have been a part of the program at the WNR. Gamma-ray measurements following neutron induced reactions are well suited to the time-of-flight (TOF) techniques used to determine the energies of the incident neutrons. The general features of the present WNR facility and TOF experiments are described by Lisowski et al.<sup>1</sup>.

In recent years three different types of detectors have been used to measure  $\gamma$ -rays in different energy ranges. High-resolution Ge detectors are used at the lowest energies and have some distinct advantages over lower resolution detectors. With Ge detectors individual reactions can be studied through identification of the final nucleus by its characteristic gamma decay. BGO crystals have a much larger detection efficiency at higher  $\gamma$ -ray energies such as those observed in capture reactions in the giant resonance region. We have extended measurements to cover the region of the giant quadrupole resonance in <sup>41</sup>Ca using a large BGO spectrometer. Still higher energy  $\gamma$ -rays are produced in neutron proton Bremsstrahlung (np $\gamma$ ) and capture reactions at high incident neutron energies. Measurements of np $\gamma$  cross sections are of interest for the information they can provide about meson exchange effects in the n-p interaction and are needed to help interpret  $\gamma$ -ray emission in heavy ion reactions as well.

In the next section we describe the characteristics of these three detector systems. In section 3 we discuss some of the experiments that have been performed with each of these detector systems and give some examples of the results obtained.

## 2. Detector Characteristics

The three most important characteristics for our measurements are the energy resolution, the time resolution, and the detection efficiency. Table 1 lists these parameters for typical detectors and experimental conditions under which we operate. The time resolution is important because it and the flight path length determine the neutron energy resolution of the experiment. To compensate for the poorer time resolution of the Ge detectors we usually perform such experiments on a 40m flight path. We compensate for the reduced flux on this longer flight path by using larger samples and larger detector solid angles. Details of the Ge detector setup are given in Ref. 2. With the BGO detectors and the  $\gamma$ -ray telescope, the good time resolution allows experiments to be performed at shorter flight path lengths, typically 18m long, where the neutron flux is greater. The energy resolution and efficiency determine the effective  $\gamma$ -ray energy range over which the detectors are useful, and the type of experiments that can be performed.

Table 1. Detector Characteristics.

Detector	$\Delta t$ (ns)	$\Delta E\gamma$ (%)	Absolute Efficiency (%)	@E $\gamma$ (MeV)	Detector Threshold
Ge	5	0.2	8	1.33	Full Energy Peak only
BGO	1	5	85	4.44	0.5 MeV
$\gamma$ -telescope	1	30	25	100.	5 MeV

The Ge detectors we use have efficiencies in the range from 15 to 30% relative to a 7.6 by 7.6 cm NaI detector for a 1.33 MeV  $\gamma$  ray. The time resolution obtained with these detectors is 5 ns for higher  $\gamma$ -ray energies and increases with decreasing  $\gamma$ -ray energy. Much larger Ge detectors are commercially available and would improve the detection efficiency by as much as a factor of 5, however the time resolution of these larger crystals is worse than that of our smaller ones. We use n-type Ge material because of its increased resistance to neutron radiation damage effects. No appreciable degradation of the energy resolution due to neutron damage has been observed in detectors operated over periods of 6 months or more at our facility. To achieve good timing with Ge detectors the constant fraction discriminator is operated in a slow risetime rejection mode. This mode reduces the observed efficiency. An alternate procedure to correct the timing without loss of efficiency is given in Ref. 3. We operate the detectors at an instantaneous count rate of 10 kHz during a beam burst. This reduces problems of degraded energy and time resolution and of excessive pulse pileup. The big advantage of Ge detectors is that their excellent  $\gamma$ -ray energy resolution simplifies the analysis and allows information to be obtained on specific reactions. Because the full energy peak for individual  $\gamma$ -rays can usually be separated from the background and from surrounding  $\gamma$ -rays, background subtraction is relatively simple and unfolding of the spectra is unnecessary. The decrease in efficiency at higher energies limits the use of these detectors to energies below 10 MeV.

We have used a spectrometer consisting of five 7.6 by 7.6 cm BGO crystals<sup>4</sup> and a much larger actively and passively shielded 10 by 15 cm BGO crystal on a rotating stand.<sup>5</sup> A diagram of the large BGO detector is shown in Fig. 1. The advantages of BGO for  $\gamma$ -ray detection are its good time resolution and good efficiency for higher energy  $\gamma$ -

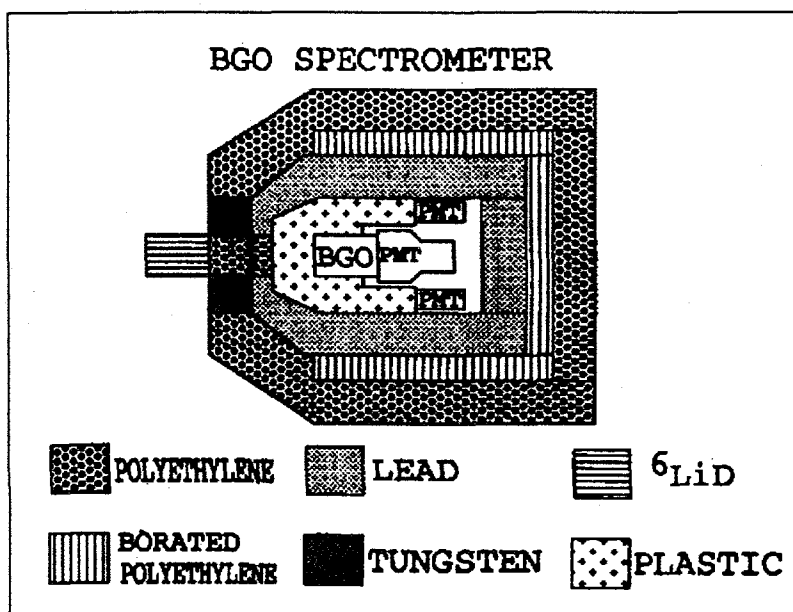
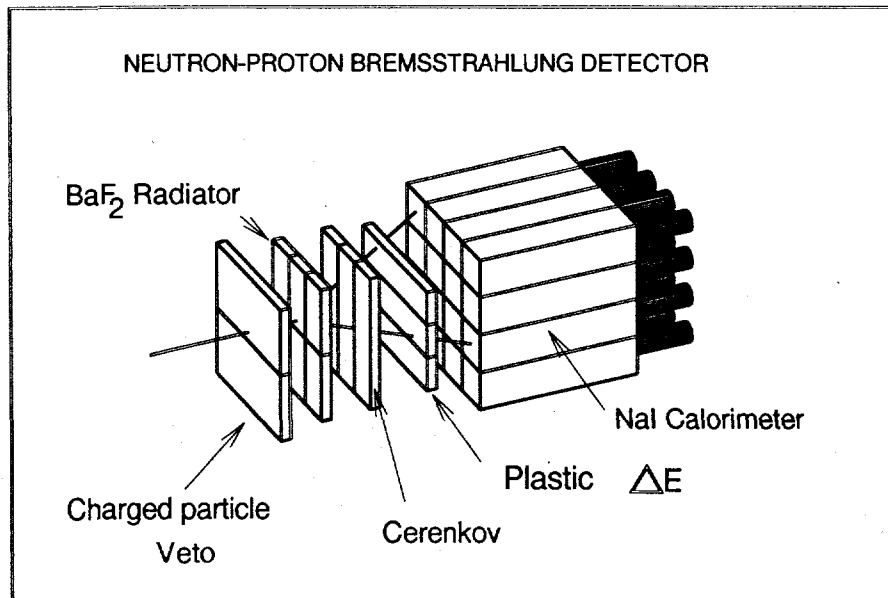


Figure 1. Diagram of the 10 by 15 cm BGO detector with active and passive shielding.

rays. The disadvantages are the poorer  $\gamma$ -ray energy resolution and the difficulty in separating backgrounds produced by neutrons from the  $\gamma$ -ray data. The larger detector has been used to measure  $\gamma$ -rays from neutron capture with energies up to 52 MeV. For this measurement the neutron background was not a problem due to the large positive Q-value for the reaction studied. The smaller BGO detectors have been used to measure angular distributions and photon production cross sections for C and N. The neutron background subtraction is accomplished by measuring neutron scattering from Be and normalizing the spectra in the correct kinematic range using the elastic scattering cross sections available in ENDF B-VI.<sup>6</sup> This technique is limited to neutron energies below approximately 20 MeV because of the energy range limits in the evaluated nuclear data files.

We constructed a large  $\gamma$ -ray telescope<sup>7</sup> similar in design to one described by Bertholet et al.<sup>8</sup> A schematic diagram of the telescope is shown in Fig. 2. The telescope arrangement provides excellent neutron rejection, and has good efficiency for  $\gamma$  rays with energies greater than approximately 40 MeV. The fast plastic and BaF<sub>2</sub> elements on the front give excellent time resolution. The energy resolution is rather poor, about 30% at 200 MeV due in part to the segmented construction with thin steel walls between the NaI elements. Unfolding of spectra from these detectors is necessary. Because this detector relies on pair production as the method of detection the efficiency drops rapidly below  $E_\gamma = 40$  MeV.



**Figure 2.** Schematic diagram of the  $\gamma$ -ray telescope. The individual NaI elements measure 10 by 10 by 40 cm. Timing, position, and particle-type information are used to select positron-electron pairs produced in the radiator.

### 3. Experiments and Results

#### 3.1. Ge Detector Experiments

In recent years we have acquired data using two Ge detectors located at angles of 90° and 125°. These angles were chosen because at 125°  $P_2$  is zero, and at 90° the difference between  $P_2$  and  $P_4$  is a maximum. The usual expansion of the  $\gamma$ -ray angular distribution in terms of Legendre polynomials is

$$A_0(1 + a_2P_2(\cos\theta) + a_4P_4(\cos\theta) + \dots).$$

For transitions where the multipolarity is less than 2, the angle integrated cross section is exactly given by  $4\pi$  times the measured cross section. For  $2^+$  to  $0^+$  transitions where the multipolarity is 2 the angle integrated cross section is only approximated by  $4\pi$  times the measured cross section to the extent that  $a_4$  is small. As will be seen in the next section  $a_4$  is not always small. We have acquired data with Ge detectors for N, O, Al, Na,  $^{56}\text{Fe}$ , and  $^{207, 208}\text{Pb}$ . The Al and Pb data are the subject of a contribution by A. Pavlik to this meeting. Some results from the Pb data are published.<sup>9</sup>

This year we modified our setup to allow the two Ge detectors to be rotated about the sample. This was done in order to measure the angular distributions of a number of transitions in light nuclei. In particular, the  $3^-$  to  $0^+$  octupole transition from the 6.13 MeV second excited state in  $^{16}\text{O}$  to the ground state is of interest, and requires measurements at 6 or 7 angles to determine  $A_0$ ,  $a_2$ ,  $a_4$ , and  $a_6$  well. The angles selected for these measurements are: 90°, 104°, 110°, 125°, 131°, 150°, and 159°.

### 3.2. BGO Detector Experiments

The 5 crystal BGO spectrometer was used to measure  $\gamma$ -ray production from C and N. The reduction of these data is rather involved. First the data are binned in suitable neutron energy bins, and if necessary  $\gamma$ -ray pulse heights can be matched through pulse height binning. Next the reduction requires background subtractions, first of the time-random backgrounds, next of the sample out backgrounds and finally of the scattered neutron backgrounds. After background subtractions, the data are deconvoluted using response functions that have been smeared with experimentally determined resolution widths. The response functions are generated using the Monte Carlo computer program CYLTRAN.<sup>10</sup> After unfolding the yields of individual peaks may then be extracted and converted to cross sections using the measured neutron fluence and the sample thickness. The detector efficiency and solid angle are included in the response function when unfolding. From the yields at the 5 angles the angular distribution coefficients can be extracted for each incident neutron energy bin. An unfolded spectrum from  $\text{N}(n, \gamma)$  is shown in Fig. 3. Figure 4 shows the angular distributions for the first excited state in  $^{12}\text{C}$  with the ENDF B-VI evaluation shown for comparison. The ENDF evaluation is based on  $\gamma$ -ray data at only two angles, and on the other available neutron scattering data. The evaluation could be improved with the inclusion of non-zero  $P_4$  coefficient data. For many if not most  $\gamma$ -ray transitions in light nuclei there is little or no data on the angular

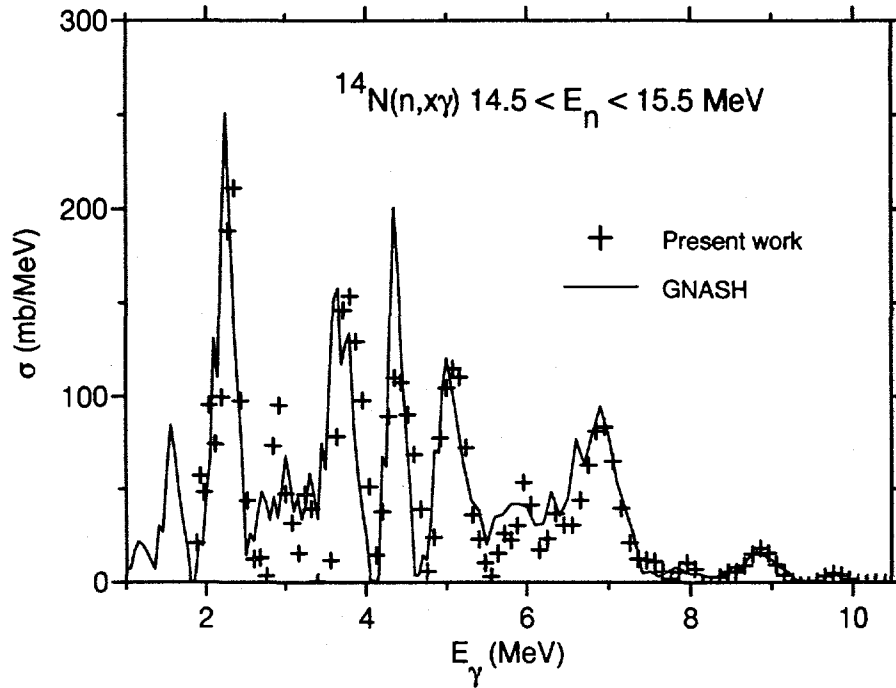


Figure 3. The  $\gamma$ -ray spectrum for  $N(n, x\gamma)$  at  $E_n = 15$  MeV. The solid line is a GNASH model calculation.<sup>11</sup>

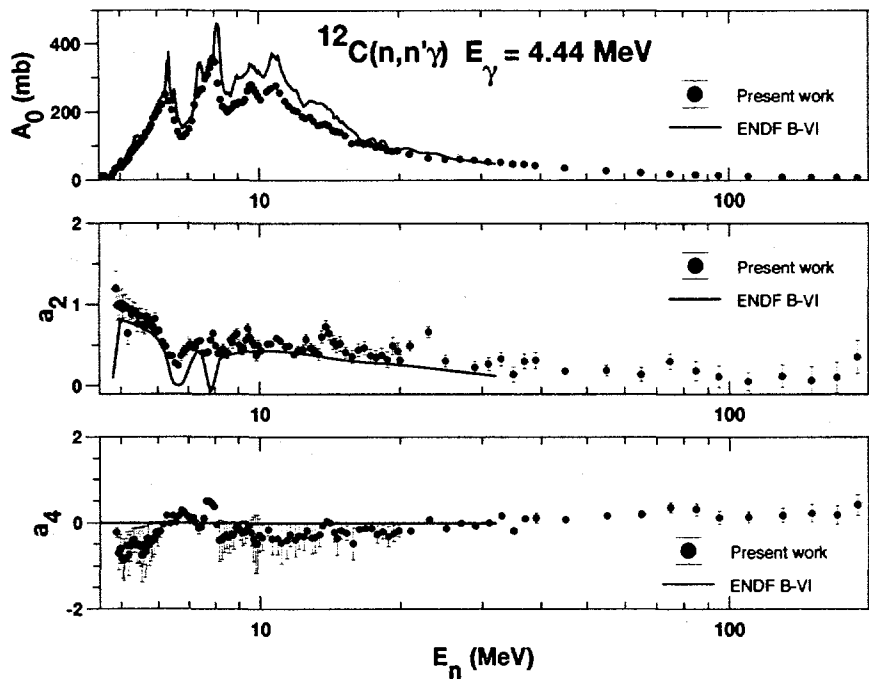


Figure 4. The excitation function for the 4.44 MeV  $\gamma$  ray from  $C(n, n'\gamma)$ . The solid line is the ENDF B-VI evaluation.

distributions of the  $\gamma$  decays. As mentioned above, due to their good energy resolution we are now carrying out such measurements with Ge detectors.

We have used a large well-shielded BGO spectrometer to measure ground state capture  $\gamma$ -rays in the  $^{40}\text{Ca}(n,\gamma)$  reaction.<sup>5</sup> The Q-value for this reaction is +8.36 MeV which places the  $\gamma$ -ray at a higher energy in the spectrum than any of the scattered neutrons. The spectrum in figure 5 shows the capture  $\gamma$ -ray peak and the neutrons and other  $\gamma$ -rays at lower energies. Extracting the contribution of capture to higher lying states is difficult using these detectors. With this detector, measurements were made at angles of  $55^\circ$ ,  $90^\circ$ , and  $125^\circ$ . From the  $55^\circ$  and  $125^\circ$  data we extracted a non-zero fore-aft asymmetry which is expected to result from the interference of the tail of the giant dipole resonance, direct capture, and the isovector giant quadrupole resonance (IVGQR). The asymmetry is shown in Fig. 6. This is the first time data have been acquired that extend higher than the peak of the IVGQR. Model fits to the data using both a direct-semi-direct model and a pure resonance model are also shown. The data in plots a and b differ only in the peak summing technique used.

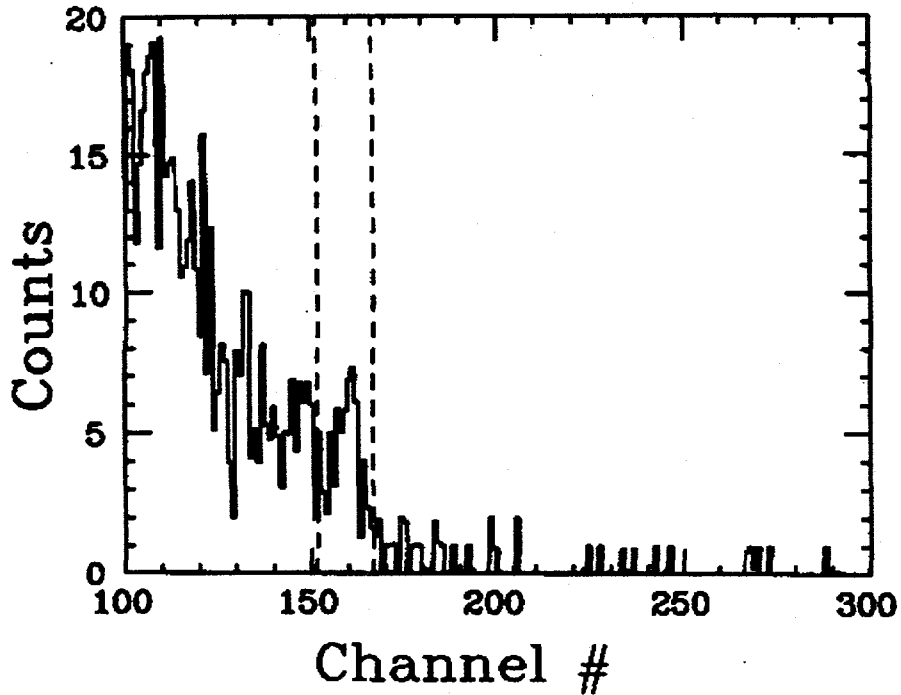
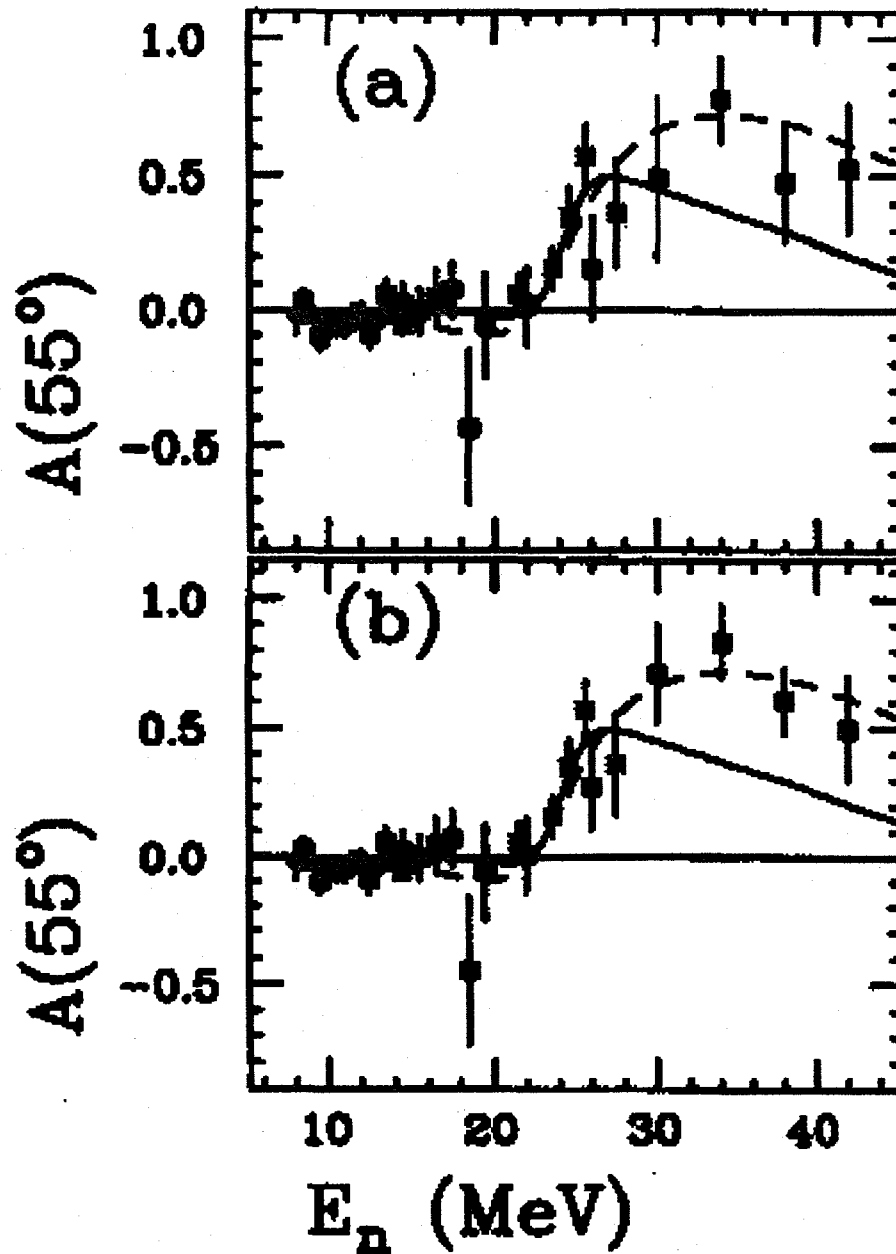


Figure 5. Spectrum at  $125^\circ$  from the  $^{40}\text{Ca}(n,\gamma)$  experiment. The dashed lines indicate the region of the peak due to  $\gamma$  rays from capture to the ground state. The data are for an incident neutron energy of 10.3 MeV and a neutron energy bin width of 50 keV. The data below the ground state capture peak include both neutron and  $\gamma$ -ray events.



**Figure 6.** The fore-aft asymmetry observed in the  $^{40}\text{Ca}(n,\gamma)$  reaction as a function of incident neutron energy. The two plots differ only in the technique used to sum the ground state capture  $\gamma$ -ray peak. The non-zero asymmetry is interpreted as due to the interference of the IVGQR with the tail of the giant dipole resonance and direct scattering. The solid line is the result of a direct semi-direct model calculation, and the dashed line is from a pure resonance model calculation.<sup>5</sup>

### 3.3. Gamma-Ray Telescope Experiments

Using a liquid hydrogen target, we have measured inclusive n $\gamma$  spectra using the  $\gamma$ -telescope described in the previous section.<sup>7,12</sup> Using a neutron energy bin 30 MeV wide around a center energy of 180 MeV, we can compare with previous data taken at a cyclotron facility<sup>13</sup>. As shown in Fig. 7 there is good agreement between the two spectra which have not been deconvoluted. The main difference between the two is that the response of the two systems is not identical. We have used similar unfolding techniques as for our BGO data to account for the response of our  $\gamma$ -telescope detector. This has the effect of shifting the peak energy higher, and changes the shape of the spectrum also. The detector response was generated using the Monte Carlo computer program EGS4<sup>14</sup>, and was verified in an experiment performed using the tagged photon facility at the Saskatchewan Accelerator Laboratory using a subset of our telescope consisting of single front converters and paddles and two of the NaI elements.

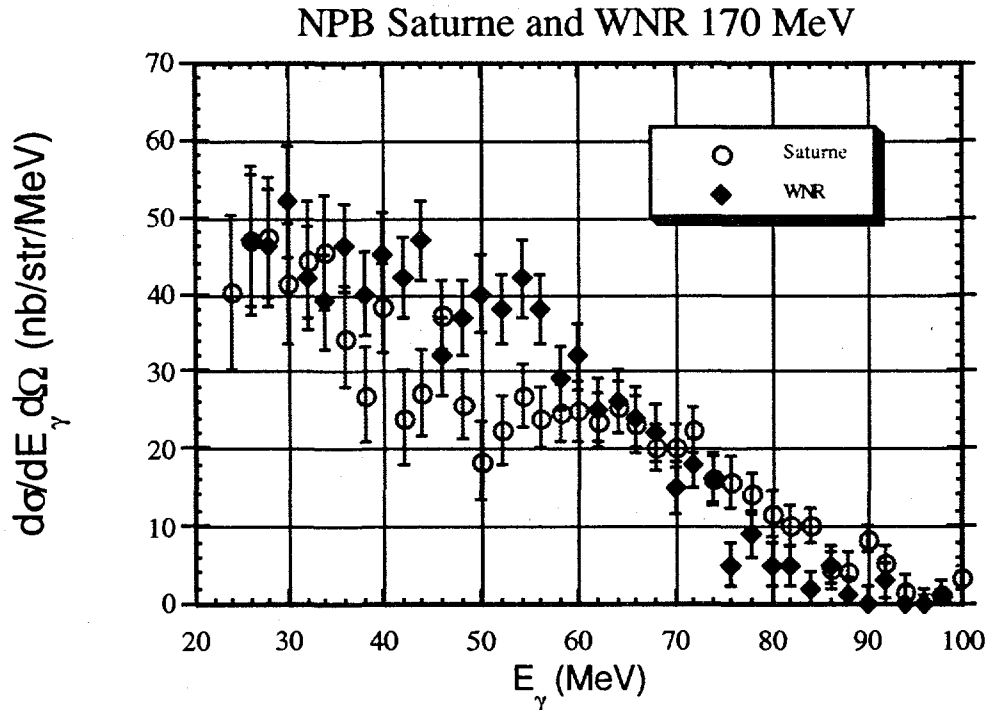


Figure 7. Inclusive n $\gamma$  spectrum for  $155 < E_n < 185$  MeV compared to the data of Ref. 12. The data have not been unfolded.

During the analysis of this experiment it became clear, based on H(n, $\gamma$ )D experiments performed at IUCF<sup>15</sup>, that the magnitude of the capture cross section was comparable to the integrated n-p Bremsstrahlung cross sections as calculated in most models. Unfolding the spectra further reinforced our belief that a large fraction of the measured spectrum

was due to capture. Most of the theories of the n $\nu$ \gamma reaction do not calculate the capture reactions contribution to the cross section explicitly, and hence should not be compared directly with the inclusive data.

The analysis of the inclusive spectra is nearing completion. In addition to being a fundamental process of interest in nuclear physics, these cross sections are necessary input for most calculations of high energy photon production in heavy ion collisions. At present we are pursuing n-p coincidence measurements to determine the differential cross sections for this three body system.

#### 4. Conclusion

Detectors have been implemented to cover the full  $\gamma$ -ray energy range available in experiments using the WNR white neutron source. The WNR facility's high-energy, broad range neutron beams enable experiments in the little-studied neutron energy range from 20 to several hundred MeV, as well as providing an outstanding facility for excitation function measurements below  $E_n=20$  MeV. We have performed experiments ranging from simple photon production cross section measurements to (n,xn $\gamma$ ) determinations of multiple neutron emission cross sections, and to the determination of the n $\nu$ \gamma cross section as a function of energy in the interesting high energy region. We continue to acquire data with the Ge detector array, and are pursuing the n $\nu$ \gamma differential cross sections using a neutron-proton coincidence setup.

#### 5. Acknowledgments

The authors should like to thank their collaborators for their support. For the n $\nu$ \gamma experiment: J.E. Koster, M. Schillaci, P.L. Anthony, M. Blann, V.R. Brown, L. Hansen, D. Krofcheck, B. Pohl, C. Sangster, F.P. Brady, J. Romero, D. Skopik, H. Nifenecker, and J.A. Pinston. For the BGO experiments: C.M. Laymon and L.R. Nilsson. For the Ge detector experiments: M.B. Chadwick, D. Drake, R.C. Haight, P.G. Young, M. Drog, H. Hitzengerger, A. Pavlik, H. Vonach, G. Bobias, and P. Englert. This work was supported by the US DOE under contract W-7405-ENG-36.

#### References

1. P. W. Lisowski, C. D. Bowman, G. J. Russell, and S. A. Wender, *Nucl. Sci. Eng.* **106** (1990) 208.
2. R. O. Nelson, C. M. Laymon, and S. A. Wender, *Nucl. Instrum. and Meth. in Phys. Res.* **B56** (1991) 451.
3. J. Kasagi, H. Ohnuma, and N. Ohyama, *Nucl. Instr. and Meth.*, **193** (1982) 557.
4. S.A. Wender, S.J. Seestrom-Morris, R.O. Nelson, *J. Phys. G* **14** (1988) S417.
5. C.M. Laymon, R.O. Nelson, S.A. Wender, and L.R. Nilsson, *Phys. Rev. C* **46**, 1880 (1992).

6. ENDF/B-VI, *The Evaluated Nuclear Data File*, Data received from National Nuclear Data Center, Brookhaven National Laboratory (1994).
7. J.E. Koster, et al., *Nucl. Instrum. and Meth. in Phys. Res.* **B79**, (1993) 297.
8. R. Bertholet, et al., *Nucl. Phys.* **A474**, (1987) 541.
9. H. Vonach, A. Pavlik, M. B. Chadwick, R. C. Haight, R. O. Nelson, S. A. Wender, and P. G. Young, *Phys Rev. C* **50** (1994) 1952.
10. J.A. Halbleib, Sr. and W.H. Vandevender, *Sandia Laboratories Report*, SAND-74-0030, 1974
11. P. G. Young, E. D. Arthur, and M. B. Chadwick, *Los Alamos National Laboratory Report* LA-12343-MS, Los Alamos, 1992.
12. D.R. Mayo, F.P. Brady, J. Romero, J.E. Koster, R.O. Nelson, M.E. Schillaci, S.A. Wender, D. Krofcheck, M. Blann, V.R. Brown, P.L. Anthony, B. Pohl, L. Hansen, C. Sangster, H. Nifenecker, J.-A. Pinston, D. Skopik, *Bull. Am. Phys. Soc.* **37**, (1992) 1257.
13. F. Malek, et al., *Phys. Lett.* **B266** (1991) 255.
14. W.R. Nelson, H. Hirayama, and D.W.O. Rogers, *Stanford Linear Accelerator Center Report*, SLAC-265, Stanford University, Stanford, CA 1984.
15. C. Bloch, et al., *IUCF Scientific and Technical Report*, p 6, May 92 - April 93, Indiana University Cyclotron Facility, and H.O. Meyer, et al. *Phys. Rev. C* **31** (1985) 309.